Scott A. Hughes
Institute for Theoretical Physics, University of California, Santa Barbara, CA 93103
Theoretical Astrophysics, California Institute of Technology, Pasadena, CA 91125

An unusual set of orbits about extreme Kerr black holes resides at the Boyer-Lindquist radius $r = M$, the coordinate of the hole's event horizon. These "horizon skimming" orbits have the property that their angular momentum L_z *increases* with inclination angle, opposite to the familiar behavior one encounters at larger radius. In this paper, I show that this behavior is characteristic of a larger family of orbits, the "nearly horizon skimming" (NHS) orbits. NHS orbits exist in the very strong field of any black hole with spin $a \gtrsim 0.952412M$. Their unusual behavior is due to the locking of particle motion near the event horizon to the hole's spin, and is therefore a signature of the Kerr metric's extreme strong field. An observational hallmark of NHS orbits is that a small body spiraling into a Kerr black hole due to gravitational-wave emission will be driven into orbits of progressively smaller inclination angle, toward the equator. This is in contrast to the "normal" behavior. For circular orbits, the change in inclination is very small, and unlikely to be of observational importance. I argue that the change in inclination may be considerably larger when one considers the evolution of inclined eccentric orbits. If this proves correct, then the gravitational waves produced by evolution through the NHS regime may constitute a very interesting and important probe of the strong-field nature of rotating black holes.

PACS numbers: 04.30.Db, 04.70.-s, 95.30.Sf

I. INTRODUCTION

The space-based gravitational-wave detector LISA [1] is being designed to make very precise measurements of the characteristics of black hole spacetimes. One source that is particularly well-suited for such measurements is the inspiral of a small (mass $\mu = 1 - 10\,M_\odot$) compact body into a massive ($M = 10^{5-7}\,M_\odot$) Kerr black hole. Depending upon the values of M, μ/M, and the hole's spin a, such an inspiral will spend several months to several years in LISA's frequency band [2], radiating $10^5 - 10^6$ gravitational-wave cycles. By accurately measuring these cycles, LISA should be able to build a "map" [3,4] of the spacetime, testing in detail the predictions of general relativity.

As the community begins developing strategies for analyzing LISA's datastream, it is important to revisit and carefully analyze the sources one expects to measure. For extreme mass ratio inspirals, this means understanding more deeply the character of Kerr black hole orbits and the nature of gravitational radiation reaction deep in the Kerr metric's strong field. Of particular interest are features that might simplify data analysis (which is likely to be very difficult, given the many cycles that must be tracked) or that might constitute a strong signature of the spacetime. In this paper, I analyze what might be such a feature — a unique signature of the inspiral of a body through the extreme strong field of rapidly rotating black holes.

The key piece of this analysis was first discussed by Wilkins. Reference [5] contains a detailed examination of circular orbits of extreme ($a = M$)[1] Kerr black holes. (In this context, "circular orbit" means "orbit of constant Boyer-Lindquist coordinate radius".) One very interesting result given in [5] is the existence of "horizon skimming" orbits. These are circular orbits of varying inclination angle at the same coordinate radius as the event horizon, $r = M$. (Despite being at the same radial coordinate, one can show that these orbits have distinct proper separation, and in particular lie outside the event horizon; see Ref. [6], particularly Fig. 2.) An extremely interesting feature of the horizon skimming orbits is that as an orbit's inclination angle ι is increased, its angular momentum component L_z likewise increases: $\partial L_z/\partial\iota > 0$ for the horizon skimming orbits. This property holds over a sizable range of radius, out to $r \simeq 1.8M$. I will call the full set of orbits for which $\partial L_z/\partial\iota > 0$ the "nearly horizon skimming" (NHS) orbits. This defining property of NHS orbits is opposite to weak-field intuition. For example, in Newtonian theory, orbits at constant radius have $L_z = |\vec{L}|\cos\iota$ (where $|\vec{L}|$ is the same for all orbits at radius r), which decreases as ι increases.

Intuition from Newtonian theory is highly suspect in the strong field of black holes. However, the true behavior of L_z as a function of ι is qualitatively the same as in Newtonian theory over a wide range of orbital radii and spins. For

[1] I use units where $G = 1 = c$.

example, when $a = 0.95M$, $\partial L_z/\partial\iota < 0$ for all circular orbits, so there are no NHS orbits when $a = 0.95M$. It turns out that NHS orbits can only exist when $a \gtrsim 0.952412M$. This is the smallest spin for which stable orbits come close enough to the hole's event horizon that $\partial L_z/\partial\iota$ can switch sign: the property $\partial L_z/\partial\iota > 0$ arises because, very close to the black hole, all physical processes become "locked" or "frozen" to the hole's event horizon [7]. In particular, their orbital motion locks to the horizon's spin. This locking dominates the "Keplerian" tendency of an orbit to move more quickly at smaller radius ($v_{\rm Kepler} = \sqrt{M/r}$), forcing a body to actually slow in the innermost orbits. The locking is particularly strong for the most-bound orbits. As I show below, the least-bound orbits do not strongly lock to the black hole's spin until they have very nearly reached the innermost orbit. The NHS orbit's $\partial L_z/\partial\iota$ behavior follows from the fact that the most-bound orbit locks to the horizon more readily than the least-bound orbit.

This behavior could have interesting observational consequences. It has been well-understood for some time that the inclination angle of an inspiraling body increases due to gravitational-wave emission [8,9]. Gravitational waves carry L_z away from the orbit, so that $dL_z/dt < 0$. Since "normal" orbits have $\partial L_z/\partial\iota < 0$, it follows that $d\iota/dt > 0$. If $\partial L_z/\partial\iota$ switches sign, then $d\iota/dt$ will switch sign as well: an inspiraling body will evolve toward an equatorial orbit. If the change in ι is large, it could have a large effect on the gravitational waveform. For example, the spin-orbit modulation of the wave's amplitude and phase is due to motion in the θ coordinate. This modulation will be reduced as the body's θ motion reduces.

Since the size of NHS orbits is significant near the "astrophysically maximal" value $a = 0.998M$ (the value at which a hole's spin tends to be buffered due to photon capture from thin disk accretion; see Ref. [10]), astrophysical black holes might spin quickly enough for NHS orbits to play some important role. This motivates a careful analysis to see what role, if any, NHS orbits might play in gravitational-wave sources. I use the code described in Ref. [9] (which uses the Teukolsky and Sasaki-Nakamura equations [11,12] to compute the flux of energy and L_z carried away from the orbit by gravitational waves) to study how a small body's motion evolves as it spirals through the NHS region. By computing the change $(dr/dt, d\iota/dt)$ at a large number of points, it is straightforward to construct the inspiral trajectory for a small body [13]. I find that the total change in inclination angle as a body spirals through the NHS region is very small — at most, $\delta\iota \simeq 1^\circ - 2^\circ$. (See Fig. 5; note that the *shape* of the curves in this figure are independent of the values of μ and M, although the timescales strongly depend on μ and M.)

The inspiral code relies on the fact that circular orbits remain circular as they evolve on an adiabatic timescale [14–16]. It is thus explicitly restricted to the evolution of circular orbits, and cannot say anything about the evolution of eccentric orbits, which are much more realistic as LISA sources [17,18]. Based on the leading order corrections to $d\iota/dt$ seen from a post-Newtonian analysis [15], I speculate that the change in ι might be much larger when eccentric, inclined orbits evolve through the strong field. Verifying this, however, will require a strong-field radiation reaction formalism that can evolve generic Kerr orbits: orbits that are inclined *and* eccentric. Such a formalism may need to be based on a local radiation reaction force [19], although recent discussion suggests it may be possible to evolve generic orbits using gravitational-wave fluxes alone [20]. The possibility that inspiral through the extreme strong field may leave an observationally significant imprint on the system's gravitational waveform will hopefully motivate future activity and progress on this problem.

Throughout this paper, the quantities t, r, θ, and ϕ refer to the Boyer-Lindquist coordinates. A prime on any quantity denotes $\partial/\partial r$. (Note that in Ref. [9] I erroneously wrote that prime denotes d/dr.) Section II reviews the properties of circular Kerr orbits, providing formulas that are useful for describing their conserved quantities E, L_z, and Q in the very strong field. These are used in Sec. III to study the NHS orbits. The NHS orbits are developed and mapped out as functions of spin and radius in Sec. III A. Section III B then re-examines them from the viewpoint of the "zero angular momentum observer", or ZAMO. The ZAMO makes local measurements of the orbital properties, and can see that their defining behavior $\partial L_z/\partial\iota > 0$ arises due to the locking of NHS orbits to the black hole's spin. In Sec. IV, I examine the trajectory of a body that is inspiraling through the NHS region under gravitational-wave emission. Here I show the very small change in ι as the body spirals in, and argue that eccentricity might impact this result greatly. Some concluding discussion is given in Sec. V.

II. CIRCULAR ORBITS OF KERR BLACK HOLES

Geodesic orbits of a Kerr black hole with mass M and spin per unit mass a are governed by the following four equations [21]:

$$\Sigma^2 \left(\frac{dr}{d\tau}\right)^2 = \left[E(r^2+a^2) - aL_z\right]^2 - \Delta\left[r^2 + (L_z - aE)^2 + Q\right] \equiv R\,, \tag{2.1a}$$

$$\Sigma^2 \left(\frac{d\theta}{d\tau}\right)^2 = Q - \cot^2\theta L_z^2 - a^2\cos^2\theta(1-E^2) \equiv \Theta^2\,, \tag{2.1b}$$

$$\Sigma\left(\frac{d\phi}{d\tau}\right) = \csc^2\theta L_z + aE\left(\frac{r^2+a^2}{\Delta} - 1\right) - \frac{a^2 L_z}{\Delta}\ , \tag{2.1c}$$

$$\Sigma\left(\frac{dt}{d\tau}\right) = E\left[\frac{(r^2+a^2)^2}{\Delta} - a^2\sin^2\theta\right] + aL_z\left(1 - \frac{r^2+a^2}{\Delta}\right)\ . \tag{2.1d}$$

The quantities E, L_z, and Q ("energy", "z-component of angular momentum", and "Carter constant") specify a family of orbits, and are conserved along any orbit of the family. Here, $\Sigma = r^2 + a^2\cos^2\theta$ and $\Delta = r^2 - 2Mr + a^2$. Eqs. (2.1a) and (2.1b) have been divided by μ^2, and Eqs. (2.1c) and (2.1d) by μ (where μ is the mass of a small body in an orbit); E, L_z, and Q are thus the specific energy, angular momentum and Carter constant. Also, $a \geq 0$; prograde and retrograde orbits are distinguished by the orbit's tilt angle rather than the sign of the hole's spin.

A circular orbit must satisfy $R = 0$, $R' = 0$; to be stable, it also must satisfy $R'' < 0$. These conditions are met for some set of orbits everywhere outside the innermost stable circular orbit, or ISCO. The ISCO lies at [6]

$$r_{\rm ISCO}/M = 3 + Z_2 - \left[(3-Z_1)(3+Z_1+2Z_2)\right]^{1/2}\ , \tag{2.2}$$

$$Z_1 = 1 + \left[1-(a/M)^2\right]^{1/3}\left[(1+a/M)^{1/3} + (1-a/M)^{1/3}\right]\ , \tag{2.3}$$

$$Z_2 = \left[3(a/M)^2 + Z_1^2\right]^{1/2}\ . \tag{2.4}$$

The ISCO varies from $r = 6M$ for a Schwarzschild black hole to $r = M$ for an extreme Kerr hole.

At all $r \geq r_{\rm ISCO}$ there exists a family of circular orbits, each member having a different inclination angle ι. We are interested in parameterizing these orbits as functions of r and ι. Consider first the weak-field limit, $r \gg r_{\rm ISCO}$. Ryan [8] has provided formulas which, with some manipulation, give E, L_z, and Q as functions of r and ι:

$$E = 1 - \frac{M}{2r} - 2\frac{a}{M}\left(\frac{M}{r}\right)^{3/2}\cos\iota\ , \tag{2.5}$$

$$\left(L_z^2 + Q\right)^{1/2} = \sqrt{rM}\left[1 - 3\frac{a}{M}\left(\frac{M}{r}\right)^{3/2}\cos\iota\right]\ . \tag{2.6}$$

[Note there is a sign error in Eq. (7) of Ref. [8], as can be seen by taking the zero eccentricity limit of Eq. (6) of Ref. [15].] One can then get L_z from the definition of the inclination angle:

$$\cos\iota = \frac{L_z}{\sqrt{L_z^2 + Q}}\ . \tag{2.7}$$

Two features of these formulas are particularly noteworthy. First, energy monotonically increases as ι increases: $\partial E/\partial\iota > 0$ for all parameters. This turns out to be true everywhere, not just in the weak field. Second, L_z monotically decreases as ι increases provided we don't abuse the applicability of Eqs. (2.6) and (2.7): $\partial L_z/\partial\iota < 0$ except when $r/M \lesssim (6a/M)^{2/3}$. This range is not even close to the weak-field, so there is no reason to believe that this result is at all physically relevant. Nonetheless, it foreshadows the behavior of the nearly horizon skimming orbits.

Turn now from the weak field to the strong field. As is conventional [8,9,15], I will use Eq. (2.7) to define the inclination angle[2] even in this regime. The *most-bound* orbit[3] (the orbit with the smallest orbital energy) at each radius is the prograde, equatorial orbit. Its constants are given by [6]

$$E^{\rm mb} = \frac{1 - 2v^2 + qv^3}{\sqrt{1 - 3v^2 + 2qv^3}}\ , \tag{2.8}$$

$$L_z^{\rm mb} = rv\frac{1 - 2qv^3 + q^2v^4}{\sqrt{1 - 3v^2 + 2qv^3}}\ , \tag{2.9}$$

$$Q^{\rm mb} = 0\ , \tag{2.10}$$

---

[2]As discussed in Ref. [9], this angle doesn't necessarily accord with intuitive notions of inclination angle. For example, except when $a = 0$, ι is *not* the angle at which most observers would see the small body cross the equatorial plane.

[3]In this paper, the terms "most-bound", "least-bound" and "marginally-bound" describe orbits at each radius. This contrasts with the usage in, *e.g.*, Ref. [6] where these terms refer to properties of *all* orbits, regardless of radius.

where $v \equiv \sqrt{M/r}$ and $q \equiv a/M$. At fixed radius, the orbital energy increases as the tilt increases from the most-bound orbit at $\iota = 0^\circ$ to the *least-bound* orbit. The least-bound orbit's characteristics depend upon r and the black hole's spin. If $r \geq r_{\rm ret}$, where [6]

$$r_{\rm ret}/M = 3 + Z_2 + [(3 - Z_1)(3 + Z_1 + 2Z_2)]^{1/2} \ , \tag{2.11}$$

then the least-bound orbit is just the retrograde, equatorial orbit. This orbit has $Q = 0$ and $\iota = 180^\circ$; expressions for its energy and angular momentum can be found in Ref. [6]. For radii $r_{\rm ISCO} \leq r \leq r_{\rm ret}$, the least-bound orbit is the *marginally-stable* orbit: the orbit which satisfies $R = 0$, $R' = 0$, and $R'' = 0$. This orbit has the maximum allowed inclination angle $\iota_{\rm max}$ at that radius. Any orbit tilted at a larger angle is unstable to small perturbations and will quickly plunge into the black hole.

For the rest of this paper, I will focus on the extreme strong field of rapidly rotating black holes. The orbits of interest are well inside the radius of the retrograde orbit. Hence, the energy $E^{\rm lb}$, angular momentum $L_z^{\rm lb}$, and Carter constant $Q^{\rm lb}$ of the least-bound orbit will be determined by numerically solving the equations $R = 0$, $R' = 0$, $R'' = 0$.

To compute the properties of a circular orbit, pick two of its constants — *e.g.*, the orbit's radius r and angular momentum L_z — and solve $R = 0 = R'$ to find the other two. This yields the following solution for $E(r, L_z)$ and $Q(r, L_z)$ [9]:

$$E(r, L_z) = \frac{a^2 L_z^2 (r - M) + r\Delta^2}{a L_z M \left(r^2 - a^2\right) \pm \Delta \sqrt{r^5 (r - 3M) + a^4 r (r + M) + a^2 r^2 (L_z^2 - 2Mr + 2r^2)}}, \tag{2.12}$$

$$Q(r, L_z) = \frac{\left[(a^2 + r^2) E(r, L_z) - a L_z\right]^2}{\Delta} - \left[r^2 + a^2 E(r, L_z)^2 - 2aE(r, L_z) L_z + L_z^2\right] \ . \tag{2.13}$$

There is a sign choice in the denominator of Eq. (2.12). In general, only one choice is physically meaningful at a given value of r. The argument of the square root in the denominator of Eq. (2.12) goes to zero at some radius $r_{\rm branch}(a)$; the plus sign corresponds to $r \geq r_{\rm branch}(a)$, and the minus sign to $r \leq r_{\rm branch}(a)$. In Ref. [9], Eq. (2.12) was used with the plus sign only since the focus in that paper was on comparatively large radius [in all cases, $r_{\rm branch}(a)$ is close to $2M$]. In this work, since I will focus on the extreme strong field, *both* signs are needed.

Rather than using Eq. (2.12), I will avoid this sign ambiguity by starting with r and E, and re-solving the system $R = 0 = R'$ for L_z and Q. Then,

$$L_z(r, E) = \frac{EM(r^2 - a^2) - \Delta \sqrt{r^2 (E^2 - 1) + rM}}{a(r - M)} \ , \tag{2.14}$$

$$Q(r, E) = \frac{\left[(a^2 + r^2) E - a L_z(r, E)\right]^2}{\Delta} - \left[r^2 + a^2 E - 2aE L_z(r, E) + L_z(r, E)^2\right] \ . \tag{2.15}$$

(There exists a second solution for L_z which has a + sign in front of the Δ, but it is not physically meaningful.) Note that Eq. (2.14) does not behave well as $a \to 0$. This is because of a degeneracy in this limit: knowledge of any three of the parameters E, r, L_z, and Q suffices to determine the orbit (because of spherical symmetry). Since this paper deals with $a \sim M$, this issue is irrelevant here.

Assembling strong-field orbits now reduces to a simple recipe. First, pick an orbital radius. Allow the orbital energy to vary from $E^{\rm mb}$ [Eq. (2.9)] to $E^{\rm lb}$ (found by solving the system $R = 0$, $R' = 0$, $R'' = 0$). For each energy, find L_z and Q with Eqs. (2.14) and (2.15). Parameterize each orbit by its inclination angle ι [Eq. (2.7)]. Repeat at a new radius.

III. NEARLY HORIZON-SKIMMING ORBITS

A. Overview

Consider for a moment the extreme Kerr limit, $a = M$. From Eq. (2.3), the ISCO is located at $r = M$, which is also the coordinate of the event horizon. It is not difficult to show that there exists a set of orbits at this radius, with the parameters

$$2M/\sqrt{3} \leq L_z \leq \sqrt{2} M \ , \tag{3.1}$$

$$E = L_z/2M \ , \tag{3.2}$$

$$Q = 3L_z^2/4 - M^2 \ . \tag{3.3}$$

These are the horizon skimming orbits. They obey $\partial L_z/\partial\iota > 0$, similar to the behavior seen when the weak-field results for L_z are pushed into the very strong field. This is opposite to the typical behavior, as exemplified by the correct usage of Eqs. (2.6) and (2.7).

Focus for now on the most-bound and least-bound orbits. These orbits bound the behavior of all orbits at each radius. As described in Sec. II, it is simple to solve for $L_z^{\rm lb}$ as a function of radius, at least numerically. Doing so for $a = M$, we find that there is a region stretching to $r \simeq 1.8M$ in which $L_z^{\rm lb} \geq L_z^{\rm mb}$. The orbits in this domain have the same dynamical characteristics as Wilkins' horizon skimming orbits, so we shall call them "nearly horizon skimming" (NHS) orbits.

Figure 1 illustrates the NHS region, and contrasts it with the "usual" behavior of Kerr orbits. It plots $L_z^{\rm mb}$ and $L_z^{\rm lb}$ for black holes with $a = 0.95M$ (top panel) and $a = M$ (bottom panel). For $a = 0.95M$, the least-bound and most-bound orbits coincide at the ISCO. Moving out in radius, the most-bound orbit's L_z grows and the least-bound orbit's L_z shrinks. This makes sense intuitively, since the inclination angle of the least-bound orbit grows as we move away from the ISCO. (Eventually, it tips over completely to $\iota = 180°$, and becomes the retrograde equatorial orbit.) The lower panel of Fig. 1 shows the behavior when $a = M$. We see the horizon skimming orbits at $r = M$ and the NHS orbits stretching out to $r \simeq 1.8M$. At that point, $L_z^{\rm lb}$ and $L_z^{\rm mb}$ cross over. Moving further out in radius, they behave in the "normal" way.

There must exist some critical spin value, $0.95M < a_{\rm NHS} < M$, at which NHS orbits first come into existence. The NHS orbits are bounded by two radii, $r_{\rm ISCO}$ and $r_{\rm cross}$ [where the angular momentum of the least-bound and most-bound orbits cross: $L_z^{\rm mb}(r_{\rm cross}) = L_z^{\rm lb}(r_{\rm cross})$]. Decreasing a must decrease the size of the NHS region — $r_{\rm ISCO}$ and $r_{\rm cross}$ approach one another. The spin at which these radii coincide and the NHS region vanishes is $a_{\rm NHS}$.

Recall from Eq. (2.12) that there are two solutions for orbital energy, only one of which is usually physical. At the crossover point, however, *both* of these energies must be physical: that with the minus sign (which is larger in magnitude) gives $E^{\rm lb}$, and vice versa. When $r_{\rm ISCO} = r_{\rm cross}$ the two energies likewise coincide, since the most-bound orbit is also the least-bound orbit at the ISCO. Thus, $a_{\rm NHS}$ is the spin that satisfies

$$E_+[r_{\rm ISCO}(a_{\rm NHS}), L_z^{\rm mb}, a_{\rm NHS}] = E_-[r_{\rm ISCO}(a_{\rm NHS}), L_z^{\rm mb}, a_{\rm NHS}] \tag{3.4}$$

[where $E_\pm$ denotes the two roots given in Eq. (2.12)]. The solution to this is $a_{\rm NHS}/M = 0.952412\cdots$.

Figure 2 illustrates the change to the NHS region as spin is varied, vanishing altogether when $a_{\rm NHS}$ is reached. The size is still significant near $a = 0.998M$. This is interesting, since $a = 0.998M$ is probably the largest spin value that we can encounter in nature [10]. This opens the possibility that NHS orbits may play a role in astrophysical processes.

B. Nearly horizon skimming orbits as seen by a ZAMO

The NHS characteristic $\partial L_z/\partial\iota > 0$ can be better understood by considering these orbits from the viewpoint of the zero angular momentum observer, or ZAMO [7]. The ZAMO is the observer that corotates with the coordinate system, such that its angular velocity as seen at infinity is

$$\omega_{\rm ZAMO} = \frac{2aMr}{(r^2+a^2)^2 - a^2\Delta\sin\theta^2} \ . \tag{3.5}$$

If one imagines spacetime to be dragged into a whirlpool-like flow by the black hole's rotation, then the ZAMO is the observer who simply rides along with the flow. (In accordance with this viewpoint, Wald [22] calls the ZAMO the "locally non-rotating observer".)

The ZAMO examines orbits in its local neighborhood. This allows it to interpret the motion of a body in a strong-field orbit with special relativistic formulas. For instance, the ZAMO measures the small body to have velocity $\vec{v}$ and energy $E_{\rm local} = (1 - \vec{v}\cdot\vec{v})^{-1/2} \equiv \gamma$. This local energy is *not* a constant of the body's motion. It is related to the conserved energy by the formula [7]

$$E = \alpha E_{\rm local} + \omega_{\rm ZAMO} L_z \ , \tag{3.6}$$

where

$$\alpha = \sqrt{\frac{\Sigma\Delta}{(r^2+a^2)^2 - a^2\Delta\sin\theta^2}} \tag{3.7}$$

is the lapse function. Knowing the energy and the angular momentum of the small body then tells us the body's speed $v = \sqrt{\vec{v}\cdot\vec{v}}$ as seen by the ZAMO.

Applying Eq. (3.6) shows that a body's speed is smallest in the most-bound orbit and highest in the least-bound orbit, varying smoothly between the two. This is due to the dragging of spacetime by the hole's spin. Let us contrast the prograde and retrograde orbits, $\iota = 0^\circ$ and $\iota = 180^\circ$. The prograde orbit is moving "downstream": part of the motion needed to keep it in orbit is provided by the dragging of inertial frames. It can orbit with relatively small velocity. The retrograde orbit, by contrast, must "swim upstream": it must overcome the dragging of inertial frames on top of the motion needed to stay in orbit. It therefore is more energetic than the prograde orbit. The angle ι smoothly varies the orbit between these extremes, so that larger ι corresponds to larger energy (and larger speed).

The velocity of a body in a non-equatorial orbit has components in both the θ and ϕ directions. The θ component goes to zero, however, at the orbit's turning points $(\theta_{\rm max}, \theta_{\rm min})$, when it reverses in θ. (Formulas for computing $\theta_{\rm max/min}$ can be found in Ref. [9]; they are just the angles at which $d\theta/d\tau = 0$ [cf. Eq. (2.1b)].) At these two points, the velocity is purely along ϕ, and the body's motion is fully described by the component $v_{\hat\phi} = \vec v \cdot \vec e_{\hat\phi}$ (where $\vec e_{\hat\phi}$ is the ϕ-component of the orthonormal basis that the ZAMO uses to make measurements). Evaluating Eq. (3.6) at $\theta_{\rm max/min}$ and writing $E_{\rm local} = \gamma$ gives a condition for $v_{\hat\phi}$ at the turning points.

The top panel of Fig. 3 shows $v_{\hat\phi}(\theta_{\rm max/min})$ for the most-bound and least-bound orbits at several interesting spins. As expected, bodies move quite a bit faster in the least-bound orbit than in the most-bound orbit. Perhaps more interestingly, $v_{\hat\phi}$ becomes substantially smaller towards the innermost orbits. This is because of the "freezing" of physics near the hole's event horizon; see Ref. [7] (particularly Secs. IIC1 and IIIA4) for further discussion. Close to the horizon, a body's motion locks to the hole's spin, and it is dragged into rigid corotation. This horizon locking causes $v_{\hat\phi}(r)$ to peak at $r \sim 1.5M$: the "Keplerian" tendency of a body to move faster as it moves inward dominates at large radii (asymptoting to $\sqrt{M/r}$ in the weak field), but is overwhelmed as the body locks onto the horizon close to the hole.

Consider next the orbit's angular momentum L_z. The ZAMO sees L_z as the product of a radius of gyration ϖ and a locally measured azimuthal momentum $p_{\hat\phi}$ [7]:

$$L_z = \varpi p_{\hat\phi} = \varpi \gamma v_{\hat\phi} \ . \tag{3.8}$$

The γ factor causes $p_{\hat\phi}$ to be even more strongly peaked than $v_{\hat\phi}$; see the lower panel of Fig. 3.

The radius of gyration is a purely geometric quantity. It is just the circumference of the ZAMO's constant r, constant θ orbit, divided by 2π:

$$\begin{aligned} \varpi = \mathcal{C}(\theta_{\rm max/min})/2\pi &= \frac{1}{2\pi}\int_0^{2\pi} \sqrt{g_{\phi\phi}(r,\theta_{\rm max/min})}\, d\phi \\ &= \sqrt{\frac{(r^2+a^2)^2 - a^2\Delta \sin\theta^2_{\rm max/min}}{r^2 + a^2\cos\theta^2_{\rm max/min}}}\ \sin\theta_{\rm max/min} \ . \end{aligned} \tag{3.9}$$

This function is plotted in Fig. 4. There are no surprises here. In the most-bound orbit, ϖ increases monotically with orbital radius, asymptoting to r at large radius. The least-bound orbit is more interesting: ϖ is smaller (not surprising, since it is a tilted orbit) and is nearly flat as a function of radius, at least over the range of NHS orbits. This near flatness is due to the orbit's increasing tilt: $\theta_{\rm max/min}$ of the least-bound orbit changes such that the circumference of the ZAMO's orbit at $\theta_{\rm max/min}$ remains nearly constant.

Since L_z is just the product of the curves shown in Figs. 3 and 4, any unusual features in the behavior of L_z must arise from features in $p_{\hat\phi}$ and ϖ. Considering these two figures, we immediately see why NHS orbits have $L_z^{\rm lb} > L_z^{\rm mb}$: the least-bound orbit has so much more linear momentum than the most-bound orbit that it compensates for its smaller radius of gyration. The linear momentum is so much larger, in turn, because the most-bound orbit is strongly locked to the spin of the black hole. The least-bound orbit is also locked for r very close to $r_{\rm ISCO}$. However, it does not lock as strongly: being so energetic, the least-bound orbit only locks as the very innermost orbits are approached. Hence, NHS orbits exist because very close orbits are forced to move in rigid corotation with the event horizon.

IV. APPLICATION: EVOLUTION UNDER GRAVITATIONAL-WAVE EMISSION

As discussed in the Introduction, binary systems consisting of a small body spiraling into a massive black hole are one of the more anticipated sources of gravitational waves for space-based detectors such as LISA. The NHS region is still rather large for $a \simeq 0.998M$ (cf. Fig. 2), indicating that there might be plenty of time for the properties of NHS orbits to influence the gravitational-wave signal of these sources.

In the extreme mass ratio, radiation reaction should operate adiabatically. In other words, the timescale for gravitational-wave emission to change an orbiting body's parameters (r, E, L_z, Q) should be significantly longer than an orbital period: $T_{\rm orb}/\tau_{\rm GW} \ll 1$. (More careful discussion of this point can be found in Ref. [9].) Because the change in these constants is very slow, the body's motion is well-approximated as geodesic over small time intervals. It is thus useful to regard the body's true, radiatively evolving trajectory as motion through a sequence of geodesic orbits. For circular orbits, we regard the body's inspiral trajectory as the evolution of its radius and inclination angle.

A simple argument shows that a body spiraling through the NHS region should behave rather differently from a body spiraling through "normal" orbits. At a given moment, a circular orbit can be represented as a point on the (r, L_z) plane. For example, a point on either the top or the bottom panels of Fig. 1 lying between the most-bound and least-bound orbit curves represents a physically allowed orbit. Radiation reaction will tend to drive this point downward and to the left in this figure: gravitational-wave emission shrinks an object's radius and reduces L_z. For a "normal" orbit, as in the top panel of Fig. 1, the body is pushed toward less-bound orbits, increasing ι. This behavior was predicted by weak-field calculations [8,15] and was recently confirmed in the strong field [9]. The evolution is in the opposite direction inside the NHS region — radiation emission pushes the body toward the sequence of most-bound orbits, so that ι decreases.

Decreasing inclination angle could have important consequences for the gravitational-wave signal. Inclined circular orbits emit waves characterized by harmonics of $\Omega_\phi = 2\pi/T_\phi$ and $\Omega_\theta = 2\pi/T_\theta$ (where T_ϕ is the period of a full range of ϕ motion, and T_θ is the period of θ motion) [9]. Roughly speaking, the θ motion modulates the gravitational waveform. The waves emitted by a body in an equatorial orbit, on the other hand, depend only on Ω_ϕ — there is no motion in θ, so the amplitudes of Ω_θ harmonics vanish. As the orbiting body moves toward the equatorial plane, the importance of the Ω_θ harmonics decreases, simplifying the waveform. Observing such simplification would be a clear signal that the small body is evolving toward the equatorial plane.

A rigorous analysis of NHS evolution requires a radiation reaction formalism good deep in the strong field. Such a formalism, specialized to the adiabatic evolution of circular orbits, is given in Ref. [9]. The code described there solves the Teukolsky equation [11] to calculate the flux of E and L_z to infinity and down the event horizon. It then applies the proof that circular orbits remain circular (changing only their radius and inclination angle) when they evolve adiabatically under radiation emission [14–16] to compute the change in Q. From this information, it is simple to obtain the change in r and ι. By computing dr/dt and $d\iota/dt$ at a large number of points, it is not difficult to compute the inspiral trajectory followed by a body that starts in an inclined, circular orbit. An algorithm and code for computing such trajectories will be presented at a later date [13].

Figure 5 shows some trajectories in the NHS region for the inspiral of a $1\,M_\odot$ compact body into a $10^6\,M_\odot$ Kerr black hole. The hole has spin $a = 0.998M$. The inspiral time for most trajectories is significant. The number of orbits around the spin axis of the black hole by the body varies from $N_\phi \simeq 73000$ for the inspiral beginning at $\iota = 0°$ to $N_\phi \simeq 400$ for the inspiral beginning at $\iota = 40°$. The number of gravitational-wave cycles is roughly proportional to N_ϕ, indicating that waves from the NHS region could contribute substantially to a measured signal. The inspiral duration scales with M^2/μ, and the number of orbits with M/μ. These quantities should be of interesting magnitude for a reasonably wide range of masses, at least for spin $a = 0.998M$. (As the spin of the black hole is dialed down to $a = a_{\rm NHS}$, the NHS orbits lose significance and inspiral through them becomes irrelevant.) Gravitational waves produced in the NHS region will form a significant part of the data measured from inspirals into rapidly rotating black holes.

Figure 5 also indicates that the signature of NHS inspiral is not very large. Although ι does decrease, as expected, the degree of decrease is quite small. For the inspirals shown, the largest change in ι is for the trajectory that starts at $\iota = 25°$: the final inclination is $\iota = 23.8°$. The change $\delta\iota = 1.2°$ is a rather paltry effect, not at all a robust signature of the strong field.

It seems that the unique signature of orbital evolution through the NHS region is not likely to be of observational interest. Before dismissing the idea entirely, let us speculate for a moment on how eccentricity might affect this conclusion. Using a weak-field radiation reaction force, Ryan has calculated the leading order evolution of the parameters of an inclined, eccentric orbit of a Kerr black hole due to gravitational-wave emission [15]. His results indicate that the eccentricity e can significantly magnify the rate at which ι changes:

$$\left.\frac{d\iota}{dt}\right|_{e\neq 0} = \left(1-e^2\right)^{-7/2}\left(1+\frac{73}{24}e^2+\frac{37}{96}e^4\right)\left.\frac{d\iota}{dt}\right|_{e=0} . \tag{4.1}$$

This relation is derived under the assumption that $r \gg M$, so there is no reason to believe it holds in the NHS region. However, it could be indicative of the effect that eccentricity has in the strong field. Notice that as eccentricity varies over the range $0 \leq e \leq 0.8$ (a reasonable range for sources that LISA is likely to measure [23]), the factor magnifying $d\iota/dt$ increases from 1 to about 100. One can speculate that $d\iota/dt$ will be magnified by a similar factor (at least to order of magnitude) under strong-field radiation reaction. At this time, there is no way to tell. Hopefully, strong-field

radiation reaction programs [19,20] will be able to model the evolution of generic Kerr orbits soon. If this speculation proves correct, then the gravitational-waves emitted by inspiral through the NHS region will contain a very strong signature of the Kerr metric strong field.

V. CONCLUSION

The result of this analysis is somewhat equivocal. I have shown that the "horizon skimming" orbits found by Wilkins are a subgroup of a larger family of orbits, the "nearly horizon skimming" orbits existing around any black hole with spin $a \gtrsim 0.952412M$. The signature characteristic of these NHS orbits is that, at fixed orbital radius, the z-component of orbital angular momentum increases as the orbit's tilt increases, in opposition to the "normal" behavior. This has the consequence that radiation emission, which carries angular momentum away from the orbit, tends to drive the system into an equatorial orbit — the system's inclination angle *decreases* rather than increases.

The fact that radiation emission drives these orbits toward the equator is a consequence of the motion of bodies in the strong field of Kerr black holes. As a body spirals in from large radius, its orbital speed initially increases, in accordance with Keplerian intuition that a body in a circular orbit of radius r has a speed $v = \sqrt{M/r}$. As the body gets very close to the black hole, however, its dynamics become dominated by the nearness of the hole's event horizon. All physical processes become "locked" to the hole as the horizon is approached. Eventually the motion of orbiting bodies synchronizes with the hole's spin. The least-bound orbit does not lock as quickly as the the most-bound orbit: close to the horizon, a less-bound orbit moves quite a bit faster than a highly bound orbit, not locking to the hole's spin until the very innermost orbits are reached. This effect is shown in Fig. 3.

As an inspiraling body's inclination decreases, the modulation of its gravitational waveform by the θ motion decreases. Measuring this decreasing modulation could be an observational hallmark of the Kerr strong field. Unfortunately, at the moment the most mature formalism for computing the effects of gravitational radiation reaction on the orbits of small bodies can only tackle the evolution of circular, inclined orbits. In this restricted case, the total change in inclination angle as a body evolves through the NHS region is quite small — at most, the orbital inclination changes by about $1 - 2$ degrees. Although I have not examined the effect of this change on the waveform, it is hard to imagine it will be particularly marked.

It is extremely unlikely that realistic extreme mass ratio inspirals will be circular. When such binaries initially form, their eccentricities are likely to be rather close to 1 [17,18], and remain significant by the time that the binary enters the sensitivity band of LISA. Weak field calculations suggest that the rate by which the inclination angle changes might be magnified by a rather large factor. If we take the leading order results at face value [cf. Eq. (4.1)], the change might be so strong that the orbit is driven nearly into the equatorial plane.

Because the NHS region is so deep in the strong field, however, it is a mistake to infer too much from leading order effects. Further progress will require a scheme to calculate radiation reaction in the strong field for *generic* Kerr orbits — orbits that are inclined and eccentric. This may require local radiation reaction forces [19], or a clever scheme for extracting the change in the Carter constant from the radiation flux [20]. The fact that observations might be able to detect a strong signature of the Kerr strong field will hopefully motivate future progress.

ACKNOWLEDGMENTS

This work grew out of a more general program to compute waveforms and radiation reaction sequences from extreme mass ratio circular orbit inspirals. That work, in turn, has benefitted greatly from conversations with Lior Burko, Curt Cutler, Dan Kennefick, Sam Finn, Lee Lindblom, Sterl Phinney, and Kip Thorne. The package MATHEMATICA was used to aid some of the calculations; all plots were produced using the package SM. This research was supported by NSF Grant AST-9731698 and NASA Grants NAG5-7034 and NAGW-4268 at Caltech, and NSF Grant PHY-9907949 at the ITP.

---

[1] K. Danzmann *et al.*, *LISA — Laser Interferometer Space Antenna, Pre-Phase A Report*, Max-Planck-Institut für Quantenoptik, Report MPQ 233 (1998).

[2] L. S. Finn and K. S. Thorne, Phys. Rev. D, submitted; also gr-qc/0007074.

[3] F. D. Ryan, Phys. Rev. D **56**, 1845 (1997).

[4] S. A. Hughes, to appear in the Proceedings of the 3rd International LISA Symposium; also gr-qc/0008058.
[5] D. C. Wilkins, Phys. Rev. D **5**, 814 (1972).
[6] J. M. Bardeen, W. H. Press, and S. A. Teukolsky, Astrophys. J. **178**, 347 (1972).
[7] K. S. Thorne, R. H. Price, and D. H. MacDonald, *Black Holes: The Membrane Paradigm* (Yale University Press, New Haven, CT, 1986).
[8] F. D. Ryan, Phys. Rev. D **52**, 3159 (1995).
[9] S. A. Hughes, Phys. Rev. D **61**, 084004 (2000); also gr-qc/9910091. S. A. Hughes, Erratum to Phys. Rev. D **61**, 084004, in press.
[10] K. S. Thorne, Astrophys. J. **191**, 507 (1974).
[11] S. A. Teukolsky, Astrophys. J. **185**, 635 (1973).
[12] M. Sasaki and T. Nakamura, Prog. Theor. Phys. **67**, 1788 (1982).
[13] S. A. Hughes, in preparation.
[14] Y. Mino, published Ph.D. thesis, Kyoto University, 1996.
[15] F. D. Ryan, Phys. Rev. D **53**, 3064 (1996).
[16] D. Kennefick and A. Ori, Phys. Rev. D **53**, 4319 (1996).
[17] S. Sigurdsson and M. J. Rees, Mon. Not. R. Astron. Soc. **284**, 318 (1997).
[18] S. Sigurdsson, Class. Quantum Grav. **14**, 1425 (1997).
[19] A. Ori, Phys. Rev. D **55**, 3444 (1997); Y. Mino, M. Sasaki, and T. Tanaka, Phys. Rev. D **55** 3457; T. C. Quinn and R. M. Wald, Phys. Rev. D **56**, 3381 (1997); L. Barack and A. Ori, Phys. Rev. D **61**, 061502; A. G. Wiseman, Phys. Rev. D **61**, 084014 (2000); L. M. Burko, Phys. Rev. Lett. **84**, 4529 (2000); C. Lousto, Phys. Rev. Lett. **84**, 5251 (2000).
[20] E. E. Flanagan and W. Tichy, in preparation. Also talk by W. Tichy at the 3rd International LISA Symposium, Albert-Einstein-Institut, Potsdam, Germany, July 2000.
[21] C. W. Misner, K. S. Thorne, and J. A. Wheeler, *Gravitation* (Freeman, San Francisco, 1973), Chap. 33.
[22] R. M. Wald, *General Relativity* (University of Chicago Press, Chicago, 1984), p. 319.
[23] This can be seen by taking a binary with initial parameters as described in Refs. [17,18] and using, for instance, formulas in [24] to estimate the eccentricity when the system enters the LISA frequency band.
[24] P. C. Peters and J. Mathews, Phys. Rev. **131**, 435 (1963); P. C. Peters, Phys. Rev. **136**, 1224 (1964).

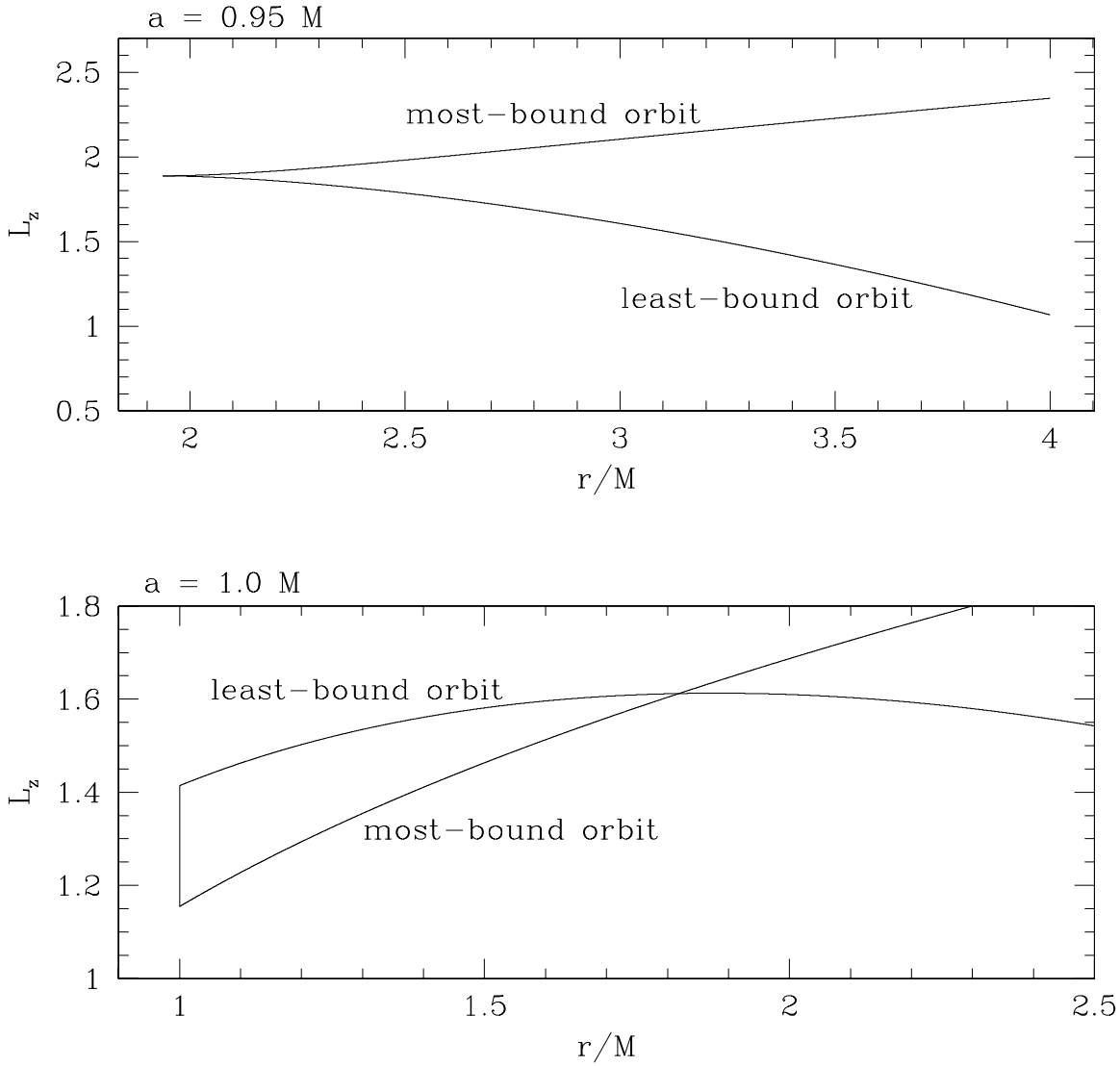

FIG. 1. Angular momentum L_z for the most-bound and least-bound circular orbits, as functions of radius. The upper panel is for $a = 0.95M$, the lower for $a = M$.

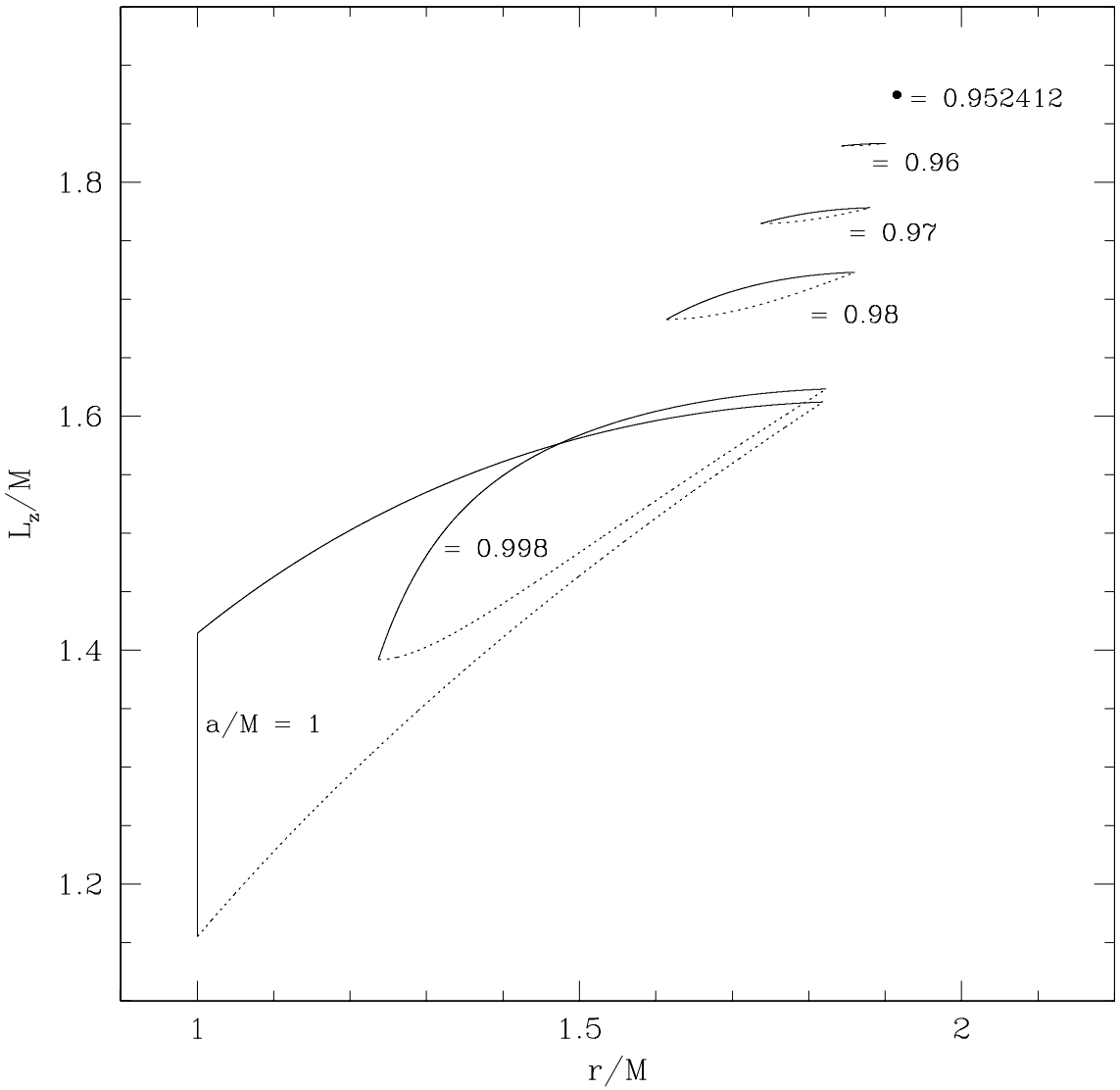

FIG. 2. The region of nearly horizon-skimming orbits for several values of the spin. The solid lines correspond to least-bound orbits, dotted lines to most-bound orbits. Notice that the region gets progressively smaller as the spin decreases from $a = M$, vanishing altogether at $a = a_{\rm crit} \simeq 0.952412M$. However, the nearly horizon-skimming region remains fairly large at least through the vicinity of $a = 0.998M$, which might apply to some astrophysical black holes.

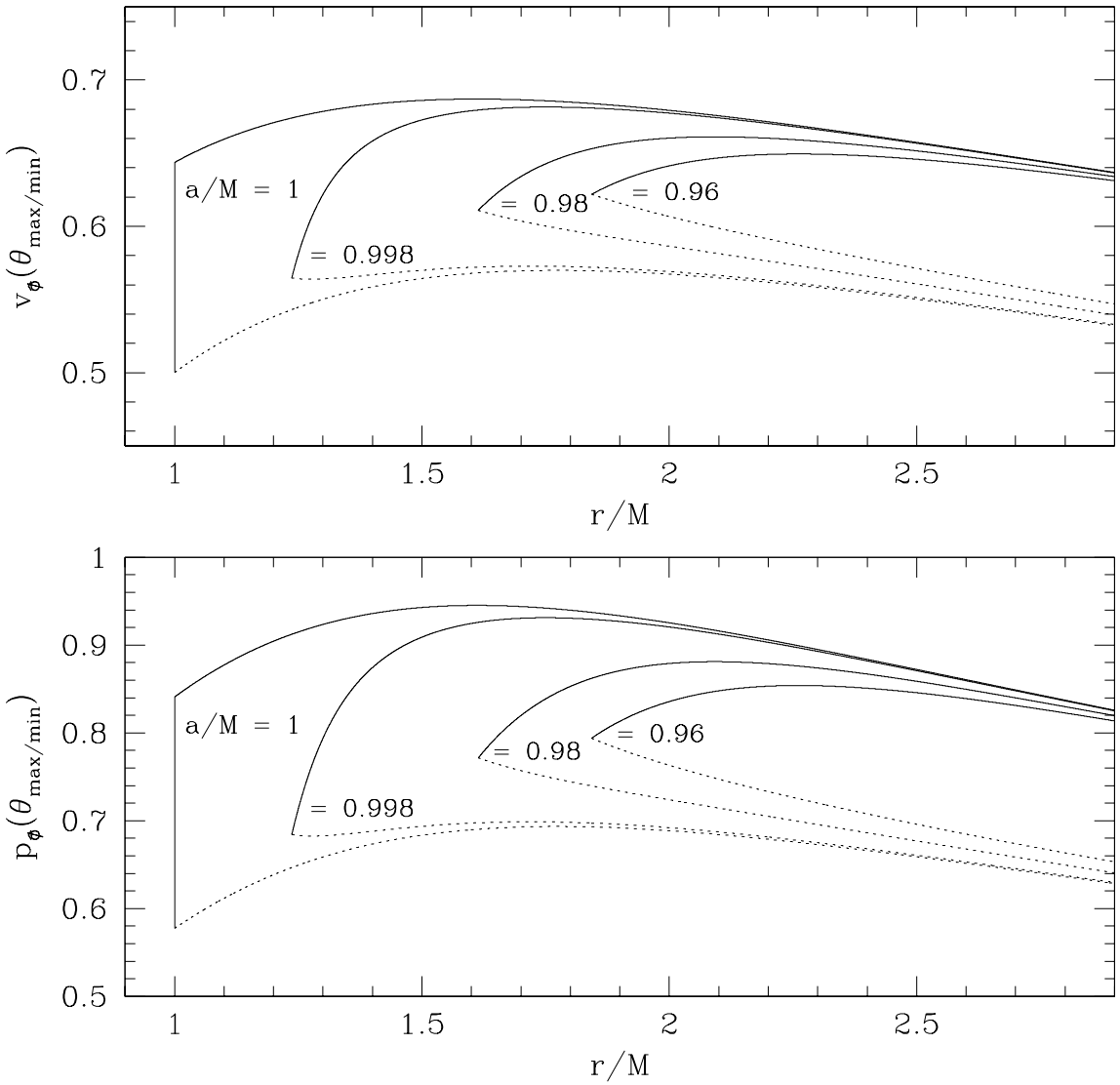

FIG. 3. The azimuthal velocity and momentum at the θ turning points of an orbiting compact body, as seen by a ZAMO. The top panel displays $v_{\hat{\phi}}$ for the most-bound orbit (dotted curve) and least-bound orbit (solid curve) at several spin values; the bottom panel likewise displays $p_{\hat{\phi}}$. As expected, a body in the least-bound orbit moves substantially faster than a body in the most-bound orbit. Notice that the motion becomes slower as the ISCO (the innermost orbit) is approached. This is because the ISCO is close to the horizon at these spin values. Orbits that come close to the horizon become locked to the rotation of the black hole. This close to the horizon, locking is substantial. This locking is reponsible for the peaks in these functions: moving inward along a sequence of orbits, a body first orbits more quickly, but then slows as its motion locks to the spin. The momentum peak is magnified (note the different vertical scales in the two panels) because $p_{\hat{\phi}} = \gamma v_{\hat{\phi}} = v_{\hat{\phi}}(1 - v_{\hat{\phi}}^2)^{-1/2}$.

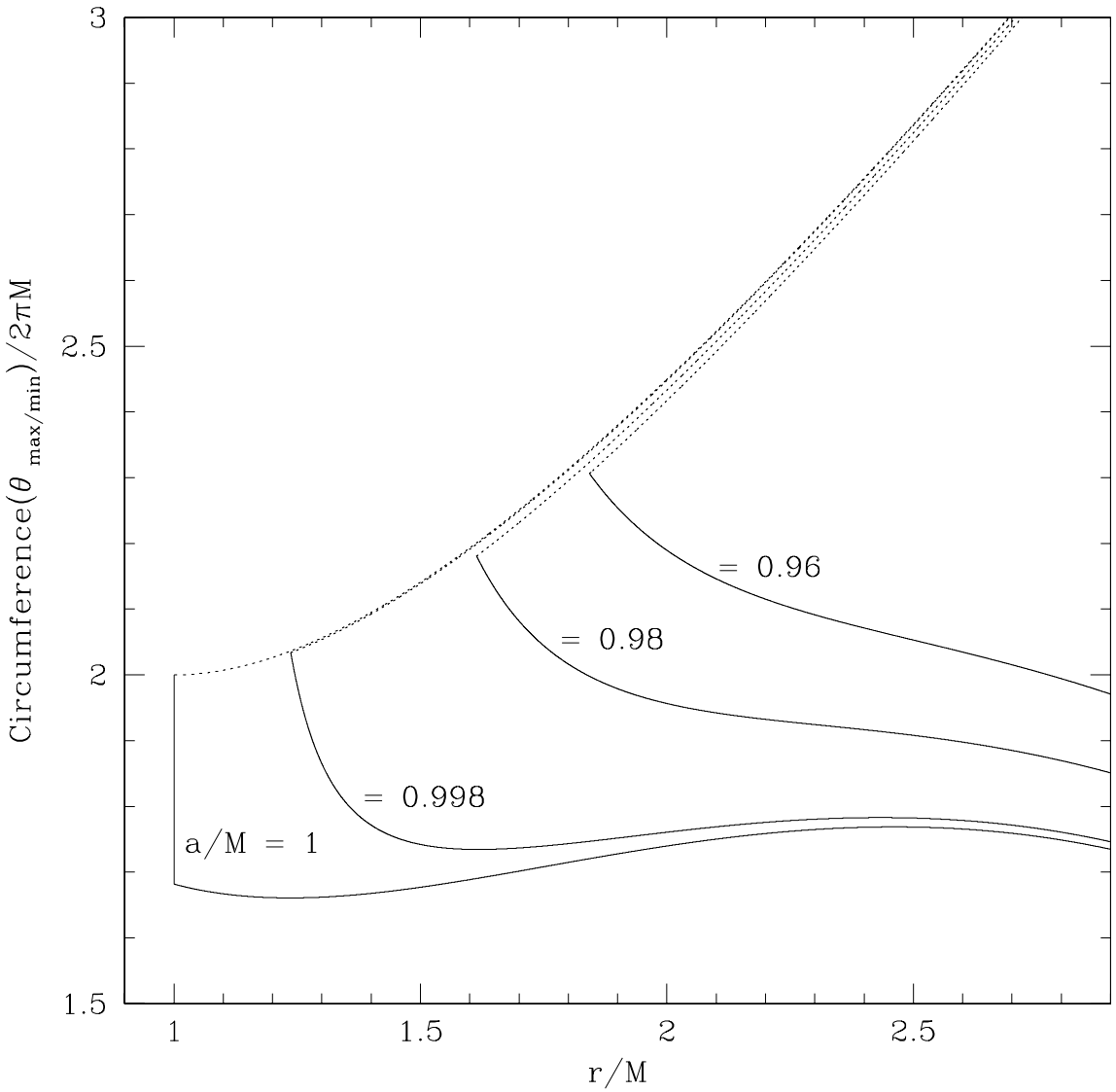

FIG. 4. The radius of gyration ϖ = Circumference($\theta_{\rm max/min}$)/2π for the most-bound orbit (dotted curve) and least-bound orbit (solid curve). Notice that ϖ barely varies for the least-bound orbit over this range. This is essentially because the change in $\theta_{\rm max/min}$ compensates for the change in radius such that the circumference of the least-bound orbit remains roughly constant.

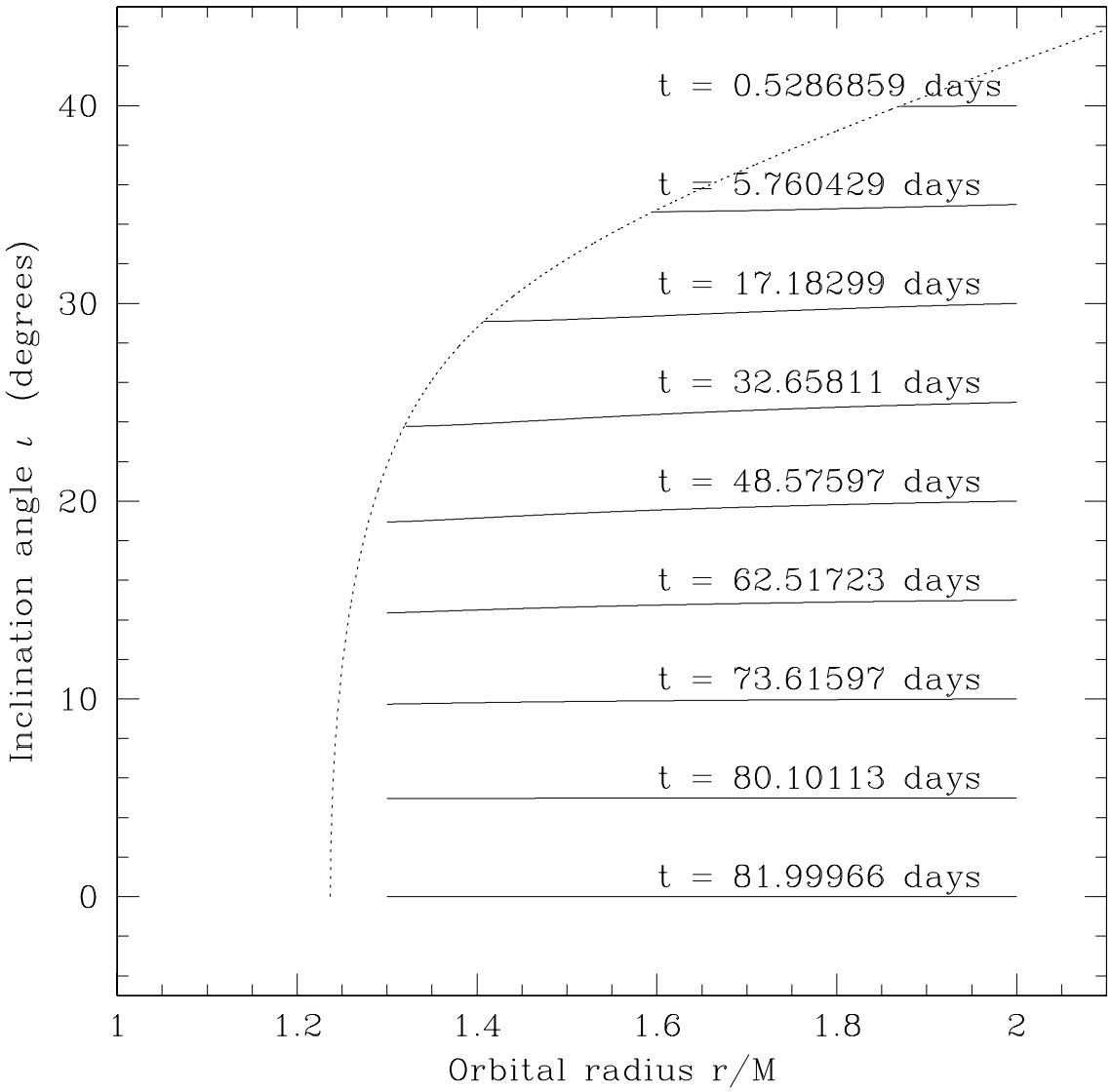

FIG. 5. The evolution of radius and inclination angle for a small body inspiraling through the NHS region. The small body has $\mu = 1\,M_\odot$, the large black hole has $M = 10^6\,M_\odot$ and spin $a = 0.998M$. The inclination angle decreases in this region, opposite to the usual behavior. The amount of decrease is, however, rather small. [The gap at the end of the inspiral trajectories for $\iota \leq 20^\circ$ is because of computational limitations: it is computationally expensive to generate a very dense mesh of $(dr/dt, d\iota/dt)$ data close to the ISCO.]